Nanostructuring of fused silica surfaces induced by KrF excimer laser radiation: Experiment and theory

P. Lorenz*, M Klöppel**, F. Frost*, M. Ehrhardt*, P. Li** and K. Zimmer*

*Leibniz-Institut für Oberflächenmodifizierung e. V., Permoserstraße 15, 04318 Leipzig, Germany

**Simulation and Optimal Processes Group, Institute of Automation & Systems Engineering, Ilmenau University of Technology, POB 10 05 65, 98684 Ilmenau, Germany

ABSTRACT

Nanostructures as well as nanoparticles have a large field of application and a growing economic importance. The usage of laser methods exhibits an outstanding potential for a fast, flexible, and cost-effective production of nanostructures. In particular, the IPSM-LIFE method (IPSM-LIFE: laser-induced front side etching using in situ pre-structured metal layers) allows the easy production of nanostructures in dielectric surfaces. In IPSM-LIFE metal layer-covered dielectric substrates are irradiated with low laser fluences. This results in the formation of complex metal structures through self-assembling processes. An additional high-energy laser irradiation of the metal–structures-covered silica causes the guided formation of complex nanopatterns in the dielectric surface.

The chromium-covered fused silica samples were irradiated by a KrF excimer laser and the structured surface was studied by scanning electron microscopy (SEM) and atomic force microscopy (AFM).

The experimental results of IPSM-LIFE are discussed with a theoretical approach considering the laser-solid interaction, the heat equation and the restructuring of the liquid film by a Navier-Stokes equation.

Keywords: nanostructuring, fused silica, excimer laser

1 INTRODUCTION

The nm-precision large-area machining of dielectric surfaces with lasers allows a fast and cost-effective fabrication of complex structures. Laser ablation [1-4] and laser etching [5-8] allow vertical nm-precison structuring. However, lateral nm-precision structuring is a big challenge for these methods. In contrast, laser-induced self-assembling processes permit the lateral nanostructuring of surfaces below the diffraction limit [9-11]. In this study, the laser-induced self-assembling and nanostructuring of thin metal layers will be used. The interaction of thin metal layers with laser radiation [12, 13] as well as the behaviour of the laser-molten metal film [14, 15] are well-known.

In this paper, the concept of the laser-induced formation of metal nanodroplets [16-18] was coupled with the principle of the LIFE process [19-23]. This method is called IPSM-LIFE (laser-induced front side etching using in situ pre-structured metal structures).

2 EXPERIMENTAL DETAILS

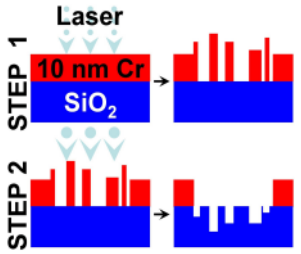

Figure 1: Schematic illustration of the IPSM-LIFE split into two different manufacturing steps:
Step 1: Generating of randomly distributed metal structures due to low laser fluence irradiation;
Step 2 Generating of nanostructures into the fused silica due to high laser fluence irradiation of the metal nanostructures.

The IPSM-LIFE process can be split into two laser manufacturing steps (see Fig. 1).

Step 1 (pre-structuring of the metal layer): The irradiation of the metal layer with low laser fluences results in a formation of randomly distributed metal nanostructures due to self assembly . The properties of the statistical distribution of the structures can be controlled by variation of the metal layer thickness, laser fluence, and pulse number.

Step 2 (structuring of dielectric surface): The irradiation of these laser-generated metal nanostructures with high laser fluences results in the nanostructuring of the dielectric surface where the resulting structures are guided by the laser-generated metal film structure

An excimer laser with a pulse duration of Δt_p = 25 ns, a wavelength of λ = 248 nm and a repetition rate of f = 10 Hz was used. The utilized laser workstation comprises beam shaping and homogenizing optics, an x-y-z positioning stage, and a dielectric attenuator and provides an energy deviation in the mask plane of below 5% rms at a square laser spot [8]. The deviation of the laser pulse energy was about 5%. Laser fluences from 60 to 600 mJ/cm² and up to

4 J/cm² were applied for step 1 and step 2, respectively. As metal/dielectric system a magnetron-sputtered chromium layer with a thickness of 10 nm and 20 nm on a fused silica substrate was used, respectively.

The treated surface was analysed by scanning electron (SEM) and atomic force microscopy (AFM).

3 RESULTS

3.1 Experimental results

(i) Step 1

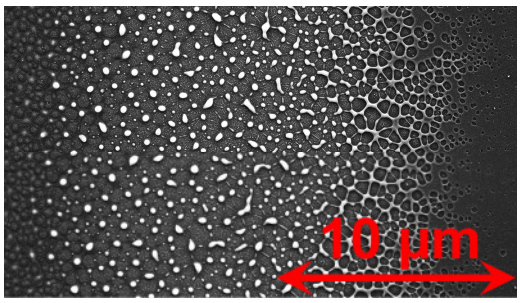

Figure 2: SEM image of an irradiated 10 nm Cr/SiO_2 sample at a pulse number N = 6 and laser fluence varying from Φ ~ 60 mJ/cm²(right) to Φ ~ 150 mJ/cm² (left).

The irradiation of a 10 nmCr/fused silcia sample results in a pronounced modification of the surface morphology where the modifications are dependent on the laser fluence (see Fig. 2) as well as on the pulse number N [24]. The irradiation with very low laser fluences (see Fig. 2, right hand side) results in a partial dewetting of the molten chromium layer on the fused silica surface and in the formation of circular holes. Higher laser fluence results in an increased diameter of the holes.

At low laser fluences, the chromium agglomerates yield to the forming of metal bars and droplets (see Fig. 3, right). The width of the metal bars decreases with increasing laser fluence. At Φ ~ 125 mJ/cm² and N = 10 metal droplets with a diameter of (350 ± 250) nm and a height of (95 ± 85) nm were detected.

At moderate laser fluences the metal bars disappear and only metal droplets were formed. Furthermore, the metal droplet size decreases due to a partial evaporation of the metal in consequence of higher temperature.

The characteristics of the nanometer metal structures depend also on the pulse number [24].

(ii) Step 2

The irradiation of the prestructured metal layer on the fused silica with high laser fluences results in an evaporation of the chromium and a partial evaporation of the fused silcia surface and finally in a nanostructuring of the dielectric surface (see Fig. 3)

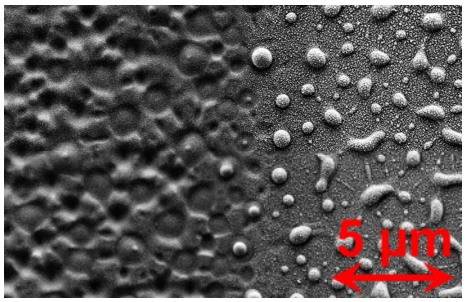

Figure 3: SEM image of an irradiated 20 nm Cr/SiO_2 sample (right) only pre-structured metal layer (Step 1: Φ_{pre} = (200 ± 50) mJ/cm², N = 5) and (left) structured fused silica surface (Step 2: Φ_{str} = (300 ± 50) mJ/cm², N = 9).

3.2 Theory

The IPSM-LIFE process is mainly dominated by two physical processes: the photon - solid interaction and the liquid film behavior.

The photon - solid interaction can be described by the heat equation (Eq. 1):

$$\rho_{M,S} \cdot c_{p;M,S} \cdot \dot{T}(t,\vec{r}_s) - \nabla(\kappa_{M,S} \cdot \nabla T(t,\vec{r}_s)) = Q(t,\vec{r}_s)$$
$$= \begin{cases} \dfrac{\Phi(\vec{r}_s,t) \cdot (1 - R_{opt})}{\Delta t_p} \cdot \alpha \cdot \exp(-\alpha \cdot z) \quad at \quad M \\ 0 \quad at \quad S \end{cases}$$

(Eq. 1)

with T: temperature, Q: laser-induced heat source, r = r(x, y, z): spatial coordinate, ρ: density, c_p: heat capacity at constant pressure, κ: thermal conductivity, α: absorption coefficient, Φ: laser-induced heat fluence and R: reflectivity (M: metal layer, S: fused silica). Further information of the used model see Ref. [25, 26].

The liquid film behaviour can be described by a Navier-Stokes equation:

$$\frac{\partial h}{\partial t^{\#}} + \nabla \cdot (h^3 \cdot \nabla(\nabla^2 h)) - \nabla \cdot (h^3 \cdot \Phi_h \cdot \nabla h) = 0$$

(Eq. 2)

with $h = h(x^{\#}, y^{\#}, t^{\#})$: non-dimensional local film thickness scaled by mean thickness Δz, $x^{\#}$, $y^{\#}$: lateral coordinates scaled by the characteristic length $(2\pi\gamma/|A|)^{1/2}\Delta z^2$, γ: surface tension, μ: viscosity, A: Hamaker constant, $t^{\#}$: normalized time scaled by $12\pi^2\mu\gamma h^5/A^2$, $\Phi_h = \left(\frac{2\pi \cdot h^2}{|A|}\right) \cdot \frac{\partial^2 G}{\partial h^2}$: excess intermolecular interactions, $G = -\frac{A}{12\pi \cdot h^2} + S^P \cdot \exp(-h/l)$: free energy, S^P: non-van-der-Waals attraction, l: correlation length. Further information see Ref. [26].

(i) Step 1

The experimental results indicate that the laser irradiation of a thin metal layer induced circular hole structures where the properties of the holes depend on the laser parameters. This process can be described by the numerical calculation of Eq. 1 and 2 [26]. The irradiation of the metal layer results in a formation of a liquid phase (Eq. 1) where the liquid phase life time depends on the laser fluences. The first estimation [26] indicates a linear dependency of the life time from the laser fluence.

$$\Delta t_{LF}^{Cr} = 0.38\,\mathrm{ns/(mJ\,cm^{-2})}\,(\Phi - 79.2\,\mathrm{mJ\,cm^{-2}}) \quad \text{(Eq. 3).}$$

Furthermore, the surface energy leads to a deformation of the film morphology (Eq. 2) and, in particular, to the formation of holes, where the expansion velocity decreases with increasing hole radius and time, respectively [26]. The radius-time dependency can be analytically described by a logarithmic function, where the maximum radius is defined by the average half distance between two holes in the order of the droplet distance (Eq. 5).

(ii) Step 2

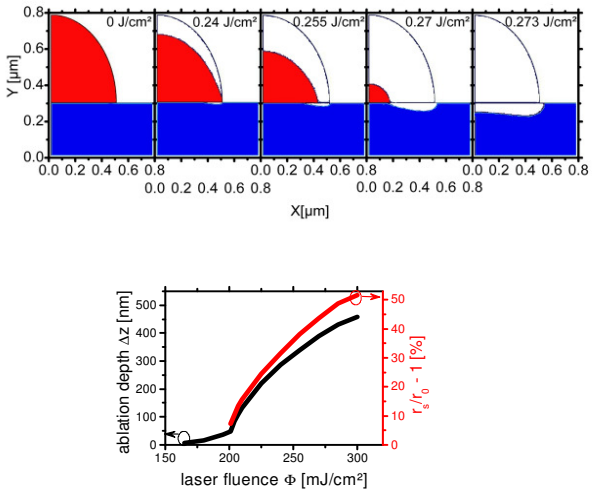

Figure 4: (top) Laser-induced ablation of the chromium/ fused silica system estimated by Eq. 1, dependent on the laser fluence which induces a determined amount of heat. (bottom) Estimated ablation depth - laser fluence dependency (black line) and increasing of the lateral outside radius of the resultant structure in fused silica (red line) (resultant outside radius r_S divided by droplet radius r_0 minus 1 in percent).

The irradiation of the pre-structured metal layer - fused silica sample with high laser fluences results in an absorption of the laser radiation by the metal structures and in a localized heating of the fused silica surface due to thermal diffusion. Finally, these effects result in an evaporation of the metal and in a partial evaporation of the fused silica surface; this process can be roughly estimated by Eq. 1 under assumption of the evaporation point of fused silica and chrome (see Fig. 4). Furthermore, this approximation allows the estimation of the resultant ablation profile in the fused silica surface dependent on the laser fluence. In Fig. 4(bottom) the resultant depht and the lateral exactness of the *structure transfer* (laterla exactness in percent is defined by resultant structure radius on the fused silica surface divided by the metal droplet radius minus 1 times 100 %) dependent on the laser fluence is displayed.

4 DISCUSSION

4.1 Step 1

The low laser fluence irradiation (Φ = 100 - 500 mJ/cm² at N = 1, Φ = 60 - 150 mJ/cm² at N=6) of the 10 nm Cr/SiO_2 system results in the formation of randomly distributed metal structures. The structure characteristics are dependent on the laser fluence Φ and on the pulse number N. Henley et al. [24] found similar effects and the formation process can be described by Navier-Stockes equation [14, 15, 25, 26] under assumption of the laser-solid interaction [26].

The theory predicted a hole formation (Eq. 4) at low laser fluences and low pulse numbers in agreement with the experimental results (see Fig. 2) where the hole radius is dependent on the laser Φ and N.

At higher laser fluences and high pulse numbers a formation of metal droplets [14, 15, 25, 26] was predicted and experimentally found (see Fig. 2 and 3).

The found results can be explained by the required dewetting time t_d (required time for the droplet formation):

$$t_d = \frac{96 \cdot \pi^2 \cdot \gamma \cdot \mu}{A^2} \cdot h^5 \quad \text{(Eq. 4).}$$

Under the assumption of a film thickness h = 10 nm, a viscosity $\mu \approx 0.000684$ kg/m*s, a surface tension $\gamma \approx 1.7$ N/m and a Hamaker parameter $A \approx 5.7*10^{-19}$ J, a dewetting time scale of $t_d \approx 0.3$ ms can be estimated. That means, under assumption of Eq. 3 at moderate laser fluences ≤ 1 J/cm² the liquid phase life time is much smaller than the dewetting time. These results are in agreement with the experimental results that the dewetting process can be *frozen* by resolidification of the metal film. This allows the found adjustment of the metal layer morphology due to the variation of the laser parameters.

Beside the variation of the metal layer due to *freezing* the resultant metal droplets (at $t \geq t_d$) are dependent on the material parameters as well as on the metal layer thickness. The average distance between two neighbouring nano-particles Λ and the diameter D of the nanoparticles can be estimated by:

$$\Lambda = \sqrt{\frac{16 \cdot \pi^3 \cdot \gamma}{A_H}} \cdot h^2 \quad \text{(Eq. 5),}$$

$$D = \left[\frac{192 \cdot \pi^2 \cdot \gamma}{A_H}\right]^{1/3} \cdot h^{5/3} \quad \text{(Eq. 6).}$$

From that, an average distance of $\Lambda \approx 4$ µm and a diameter of D ≈ 800 nm can be found.

The theoretical predicted values are a little bit too high in comparison to the experimental results (see section 3.1. (i)). This effect is most likely explained by the non-perfect estimation of the material parameters. However, the theoretical approach allows the estimation of the statistical properties of the irradiated metal layer.

4.2 Step 2

The irradiation of the Cr/SiO_2 system, with randomly distributed metal structures, results in an absorption of the laser energy in the chromium nanostructures,in an energy transfer into the dielectric surface and, finally, in an ablation process of the chromium as well as partially of the fused silica surface (see Fig. 3).

The LIFE process (direct homogenous ablation of fused silica assisted by metal layer at high laser fluences) has shown that the etching depth linearly increases with the laser fluence and exponentially with the metal layer thickness for a metal thickness of up to 20 nm [19].

For the local ablation process in the IPSM-LIFE process similar results were found: the etching depth in fused silica increased with increasing laser fluences (Φ_{str}).

Besides the increase of the etching depth also a lateral increasing of the ablation area was experimentally detected [24]. This effect can be explained by a larger vertical and lateral thermal influence zone at higher laser fluences due to higher absorbed laser energy.

Furthermore, these effects can be easily simulated (see Fig. 4) under the assumption of a thermodynamic equation (Eq. 1). The simulation shows a laser-induced localized ablation of the fused silica where the ablation depth increased with raising laser fluence as well as the transferred lateral structures increased with raising laser fluence (see Fig. 4). That means, for a lateral accurate transfer of the geometry low laser fluence is suitable. However, for a large ablation depth higher laser fluence is necessary.

5 CONCLUSIONS AND OUTLOOK

The combination of laser-induced front side etching method with in situ nanostructuring of the covering metal film allows the fabrication of complex, randomly distributed surface structures with a lateral size down to a few 10 nm into the fused silica surface.

The IPSM-LIFE process can be divided into two steps:

1. The low laser fluence irradiation results in a formation of complex, randomly distributed metal structures (see Fig. 1 step 1) by self assembly of the molten thin film. The resulting metal structure can be controlled by the fluence and the pulse number (see Fig. 2) as well as by the material parameters (metal layer and substrate).

2. The high-energy laser irradiation of these complex metal structures results in the *'guided transfer'* of the metal pattern into the substrate (see Fig. 1 step 2 and Fig. 3). The fused silica nano structures depend on the laser parameters and on the metal structure.

The IPSM-LIFE process can be theoretically described by a heat equation and a Navier-Stokes equation. The estimation allows a good qualitative description of the experimental results. For a quantitative description a coupling of the differential equation, an optimization of the material parameters as well as an assumption of the melting and evaporation enthalpy is necessary.

The next challenge for the IPSM-LIFE process is the fabrication of well-ordered, periodic structures. The modulation of the laser beam intensity profile by phase masks might be appropriate for the fabrication of ordered metal structures [28] and, finally, by exploiting the proposed method for the production of lateral and vertical nm-precision periodic complex surface structures in dielectrics.

ACKNOLEDGEMENTS

We are grateful for funding from the Deutsche Forschungsgemeinschaft (DFG).

REFERENCES

[1] P. R. Herman et al., Appl. Surf. Sci. 154–155, 577 (2000).
[2] M. Lenzner et al., Appl. Phys. A 68, 369 (1999).
[3] J. Ihlemann et al., Appl. Phys. A 54, 363 (1992).
[4] J. Ihlemann et al., Appl. Surf. Sci. 106, 282 (1996).
[5] R. Böhme et al., Laser Micro/Nanoeng. 1, 190 (2006).
[6] K. Zimmer et al., Appl. Surf. Sci. 255, 9617 (2009).
[7] M. Ehrhardt et al., Appl. Phys. A 101, 399 (2010).
[8] P. Lorenz et al., Phys. Status. Solidi A 209, 1114 (2012).
[9] Wagner et al. Appl. Surf. Sci. 252, 8576 (2006).
[10] Kuznetsov et al., Appl. Phys. A 94, 221 (2009).
[11] Ratautas et al., JLMN 7, 355 (2012).
[12] E. Matthias et al., Appl. Phys. A 58, 129 (1994).
[13] S. J. Henley et al., Phys. Rev. B 72, 195408 (2005).
[14] A. Sharma et al., Phys. Rev. Lett. 81, 3463 (1998).
[15] A. Yochelis et al., Eur. Phys. J. E 22, 41 (2007).
[16] S. Imamova et al., J. Optoelectron. Adv. Mater. 12, 500 (2010).
[17] S. J. Henley et al., Appl. Phys. Lett. 84, 4035 (2004).
[18] K. Ratautas et al., J. Appl. Phys. 112, 013108 (2012).
[19] P. Lorenz, et al., Appl. Surf. Sci. 258, 9742 (2012).
[20] P. Lorenz, et al., Physics Procedia 39, 542 (2012).
[21] P. Lorenz et al., Appl. Surf. Sci. 265, 648 (2012)
[22] P. Lorenz et al., "Laser-induced front side etching of fused silica with femtosecond laser using thin metal", Appl. Surf. Sci. – in press, DOI:10.1016/j.apsusc.2012.11.047.
[23] P. Lorenz, et al., Proc. SPIE 8243, 82430Y (2012).
24] P. Lorenz et al., "Laser-induced fabrication of randomly distributed nanostructures into fused silica surfaces" Appl. Phys. A – submitted.
[25] P. Lorenz et al., Appl. Surf. Sci. 258, 9138, (2012).
[26] P. Lorenz et al., "Laser-Induced Circular Nanostructures in Fused Silica Assisted by a Self-Assembling Chromium Layer" Appl. Surf. Sci. – submitted.
[27] S. J. Henley et al., Appl. Surf. Sci. 253, 8080 (2007).
[28] M. Mäder et al., Phys. Status Solidi B 247, 1372 (2010).